



## Observations of the ionospheric projection of the plasmopause

P. C. Anderson,<sup>1</sup> W. R. Johnston,<sup>1</sup> and J. Goldstein<sup>2</sup>

Received 18 April 2008; revised 2 June 2008; accepted 25 June 2008; published 15 August 2008.

[1] We demonstrate a method for extracting the ionospheric projection of the plasmopause (PP) from DMSP measurements of the  $H^+$  density in the topside ionosphere. The results agree well with PP locations derived from images of the plasmasphere acquired by the IMAGE spacecraft during a 72-day period in 2001. The DMSP-derived PP locations are usually earthward of the IMAGE EUV PP locations, on average about 0.5 L. The locations are also usually earthward of PP locations derived from the O'Brien and Moldwin [2003] empirical PP model, on average about 1 L. Nearly all of the cases when the DMSP-derived PP location is more than about 0.5 L different than the IMAGE-derived PP location occur during periods when the plasmasphere and PP are showing significant structure. Examination of these periods suggests that the DMSP measurements are often identifying physical structures in the plasmasphere. **Citation:** Anderson, P. C., W. R. Johnston, and J. Goldstein (2008), Observations of the ionospheric projection of the plasmopause, *Geophys. Res. Lett.*, 35, L15110, doi:10.1029/2008GL033978.

### 1. Introduction

[2] The plasmasphere is a cold corotating torus of plasma within the innermost region of the magnetosphere surrounding the Earth. The outer boundary of the plasmasphere, known as the plasmopause (PP), is very dynamic and its structure and location are highly dependent on the interaction between the electric field associated with Earth's rotation and the solar wind-induced sunward convection. An increase in magnetospheric convection can trigger plasmaspheric erosion, in which the outer layers of the plasmasphere are stripped away, and the PP moves inward – rapidly on the night side and over the course of about half a day on the day side.

[3] Many ionospheric signatures of the PP have been proposed, including the mid-latitude electron density trough [e.g., Grebowsky *et al.*, 1976; Yizengaw and Moldwin, 2005]. However, evidence for this has been elusive, largely because of the lack of simultaneous measurements. Foster *et al.* [1978] and Grebowsky *et al.* [1978] found that the lower-latitude edge of the topside ionospheric trough was typically equatorward of the PP footprint identified by whistler waves. Yizengaw and Moldwin [2005] found a good correlation between the PP and the mid-latitude trough using tomographic GPS imaging and EUV images from the IMAGE spacecraft. Taylor and Walsh [1972] noted that the

sharp latitudinal gradient in the  $H^+$  and  $He^+$  density below 1000 km (the light ion trough - LIT) was a more consistently observable feature in the mid-latitude ionosphere and proposed it as the ionospheric signature of the PP. Park and Banks [1974] performed direct intercomparison of the LIT with the PP determined by whistler wave and thermal particle measurements and showed a general agreement but not a one-to-one correspondence. Foster *et al.* [1978] found that the invariant latitude of the steep gradient in the thermal plasma density increased with altitude in the topside ionosphere and concluded that, at times, the dynamics of the coupling between the ionosphere and the plasmasphere in the topside ionosphere might have obscured the location of the PP. Grebowsky *et al.* [1978] concluded that density depletions in  $H^+$  in the topside ionosphere away from the location of the PP could result from localized depletions in  $O^+$ .

[4] The location of the PP is a crucial factor in the location and intensities of the electron fluxes in the outer radiation belt zone, which depend on a dynamic imbalance between energization and loss processes. It has been suggested that pitch-angle scattering by electromagnetic ion cyclotron (EMIC) waves and broad-band whistler mode emissions known as plasmaspheric hiss are the primary loss mechanisms for radiation belt particles while stochastic acceleration by whistler-mode chorus is a significant energization source (see review by Horne [2002]). Summers *et al.* [1998] suggest a scenario for radiation belt energization and loss that is very dependent on the location of the PP, particularly on the dusk side. Whistler mode chorus waves are excited in the region outside the PP by cyclotron resonance with anisotropic 10–100 keV electrons over a broad range of MLT values [e.g., Koons and Roeder, 1990] while electromagnetic ion cyclotron (EMIC) waves are excited by convective injection of ring current  $H^+$  ions preferentially along the duskside PP [e.g., Jordanova *et al.*, 1997]. So the loss rate and spatial distribution of relativistic electrons are highly dependent on the PP location in the dusk sector.

[5] It is quite clear that simultaneous measurements of the flux and distribution of radiation belt particles and the location of the PP over an extended period of time are critical for the development of an understanding of radiation belt dynamics. Observational studies showing the relationship of the PP and the inner extent of the outer belt have been performed [e.g., Baker *et al.*, 2004; Goldstein *et al.*, 2005], but the data only covered a limited period of time and lacked continuous PP measurements. Other comparative studies have included the PP as a statistical or modeled quantity [e.g., O'Brien and Moldwin, 2003]. We plan to address this issue using measurements of the LIT by the DMSP spacecraft from which the location of the ionospheric projection of the PP can be determined. The DMSP-derived PP locations can be used to fill in the gaps

<sup>1</sup>W. B. Hanson Center for Space Sciences, University of Texas at Dallas, Richardson, Texas, USA.

<sup>2</sup>Space Science and Engineering Division, Southwest Research Institute, San Antonio, Texas, USA.

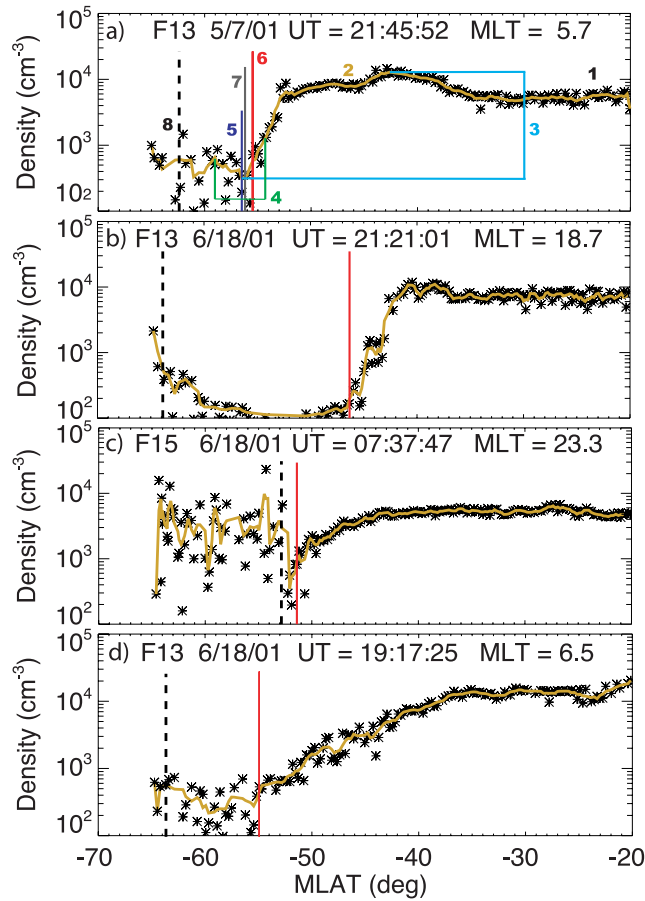


**Figure 1.**  $H^+$  density measurements from the DMSP (a, b, and d) F13 and (c) F15 spacecraft. The red vertical lines indicate our identified PP locations while the black, dashed vertical lines indicate the location of the equatorial edge of the energetic electron precipitation. The numbers 1–7 in Figure 1a refer to the steps of the PP identification procedure.

during periods when data from other spacecraft are unavailable. Such measurements have been made on 7 different DMSP spacecraft operating continuously since 1990. In this paper, we demonstrate the efficacy of using the DMSP measurements to identify the location of the PP by comparing the derived locations with those derived from the IMAGE EUV images.

## 2. Observations

[6] The DMSP spacecraft fly in sun-synchronous, dawn-to-dusk and premidnight-to-noon orbits at  $\sim 840$  km altitude with  $\sim 99^\circ$  inclinations and orbital periods near 101 min. Figures 1a–1d show the  $H^+$  densities measured by the Retarding Potential Analyzer (RPA) on board the DMSP F13 and F15 spacecraft at several MLT locations. The red vertical lines indicate our identified PP locations. The black, dashed vertical lines indicate the location of the equatorial edge of the energetic electron precipitation determined from data from the on-board SSJ/4 spectrometer that allows us to unambiguously determine that the spacecraft is observing the region equatorward of the plasmasheet.

[7] The procedure for boundary identification is illustrated in Figure 1a; the numbers 1–7 refer to the steps of the procedure. For each DMSP pass, we plot the  $H^+$  density data [1] between  $20^\circ$  and  $65^\circ$  magnetic latitude (MLAT) and take a 5-point smooth [2]. If the dynamic range [3] of the resulting series is less than a factor of 10, the pass is automatically rejected; some remaining passes are also manually rejected at this point on the basis of factors such as very noisy data or no evident LIT. For each pass that is analyzed, a range of MLAT near the LIT density minimum is manually specified [4], and the routine identifies the density minimum in this range [5]. Proceeding equatorward from this minimum, the LIT boundary is selected as that point [6] where the smoothed density reaches a value of a factor of 1.5 times the density value at the identified minimum. This factor of 1.5 was based on analysis of typical trough gradients; the difference in MLAT between the density minimum and selected PP position for all of the  $>1700$  PP identifications in this study is  $1.16^\circ \pm 0.68^\circ$  MLAT. A boundary is also manually selected [7] at the poleward side of the LIT gradient, where the slope of the gradient drops to a low value and before the noisy density data associated with the auroral zone/polar cap begins. If the location selected by the routine [6] is separated from this manually selected boundary [7] by more than  $2^\circ$  in MLAT or otherwise discordant (i.e., if noise in the data warranted rejection at an earlier stage), it is rejected.

[8] The ionospheric projection of the PP is not always identifiable in the DMSP data as a trough must be present and the  $H^+$  density must be greater than about 5% of the total density to retrieve it accurately from the RPA data analysis. During solar maximum in the summer hemisphere and on the dayside, photoionization production of  $O^+$  can dominate the charge exchange reaction of  $O^+$  with neutral H (the primary source for  $H^+$  in the ionosphere) and the  $H^+$  density can be less than 5% of the total. All but 5 of the  $>1700$  PP identifications presented in this paper occurred when the solar zenith angle was greater than  $95^\circ$ , so there are almost no PP identifications on the dayside. With up to four satellites in orbit at once, providing continuous data on 14.5 orbits a day, there are up to over 200 possible PP crossings a day. This allows us to discard any ambiguous data without concern about a lack of observations.

[9] Figure 2 shows images of the equatorial distribution of the 30.4 nm solar radiation resonantly scattered by plasmaspheric  $He^+$  acquired by the IMAGE EUV instrument versus X and Y in SM coordinates. The PP is assumed to be where the brightness of the emissions drops abruptly and is associated with an  $He^+$  density threshold of about  $30\text{--}50\text{ cm}^{-3}$  during quiet times and somewhat higher during intense geomagnetic activity. The derivation of the PP boundary from the EUV data has been described numerous times in the literature [e.g., Goldstein *et al.*, 2003, 2005].

[10] The red traces show the DMSP F13 and F15 orbit tracks mapped to the equator in SM coordinates using the IGRF 2000 internal magnetic field model combined with the Tsyganenko 2001 external magnetic field model. The red crosses indicate the location of the ionospheric projection of the PP as inferred from the DMSP  $H^+$  measurements and the white circles indicate the PP identified in the IMAGE data. The boundaries agree remarkably well, with

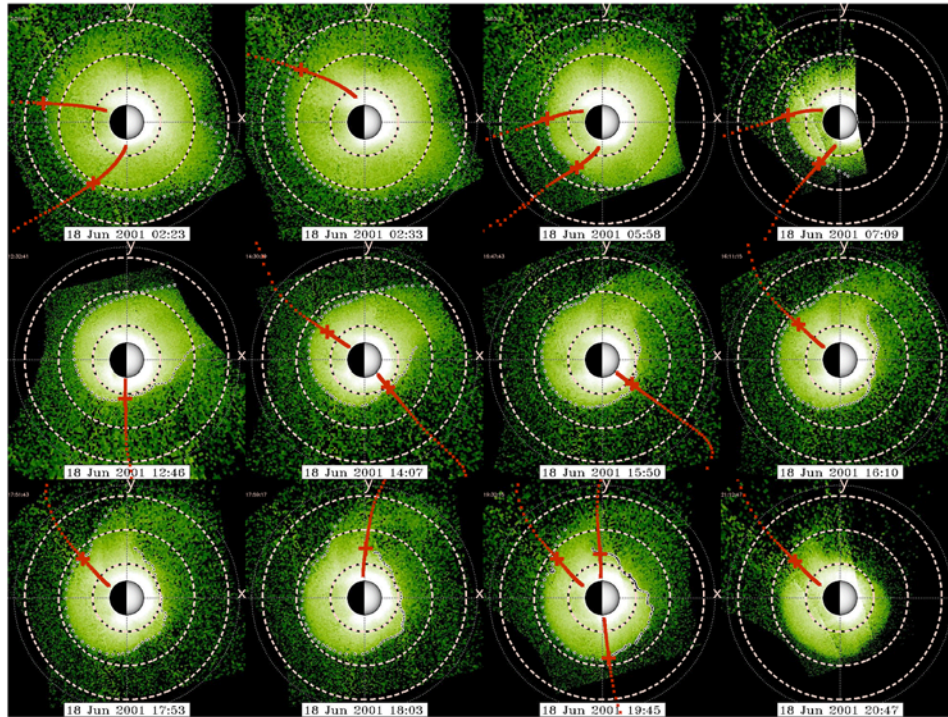


**Figure 2.** IMAGE EUV observations of the plasmaspheric  $\text{He}^+$  density on 18 June 2001. Each panel shows the equatorial  $\text{He}^+$  distribution versus  $X$  and  $Y$  in SM coordinates. The Sun is to the right, dusk is to the top, and circles are drawn at  $L = 2, 4, 6,$  and  $6.62$  (geosynchronous orbit). The red traces show DMSP F13 and F15 orbit tracks mapped to the equator in SM coordinates. The red crosses indicate the location of the ionospheric projection of the DMSP-inferred PP.

the greatest disagreement occurring for the image at 14:07 UT, where the boundaries disagree by about  $1 R_E$ .

[11] Applying our method to a 72-day period during 2001 (days 80–151), we obtained 1790 PP identifications or an average of 25 identifications per day representing about 12% of all possible PP crossings. The number of identifications per day varied from 0 (1 day) to 47. We then made quantitative comparisons of the DMSP and IMAGE PP identifications.

[12] We identified all DMSP-derived PP locations acquired within 15 minutes UT of an EUV image and derived an IMAGE-based  $L$  value ( $L_I$ ) by averaging the IMAGE PP points within 15 minutes of MLT of the DMSP identification giving 187 comparisons. Figure 3a shows a comparison of  $L_I$  and the DMSP PP  $L$  values ( $L_D$ ). The error bars show the variation in  $L_I$  over the 15 minutes of MLT surrounding the DMSP MLT at the identified  $L_D$ . We identified all comparisons where  $(L_I - L_D)/L_I$  was greater/less than 0.41 (open/solid circles). This separated the results into two clusters. This was not meant to be quantitative but to give us an idea of which comparisons were “bad”; examples of these will be discussed later. There were 145 points in the “good” cluster (78% of the sample) with a mean difference in  $L$  value of  $0.435 \pm 0.407$ , and 42 points in the “bad” cluster (22% of sample) with a mean difference in  $L$  value of  $1.770 \pm 0.440$ . Most of the sample then is in the cluster where the DMSP PP is on average 0.435  $L$  inward of the IMAGE PP. Given that the error in the IMAGE-extracted PP is  $<0.25 L$  [Goldstein *et al.*, 2005], this difference is not unreasonable. The solid line represents a one-to-one correspondence while the dashed line is a fit to the

“good” cluster. The equation of the dashed line is  $L_I = 0.914L_D + 0.729$ ; the correlation coefficient is 0.71.

[13] O’Brien and Moldwin [2003] developed an empirical PP model parameterized by both Dst and MLT. For the 1790 PP identifications from the 72-day case study, we have calculated PP  $L$  values from the O’Brien-Moldwin model ( $L_{OM}$ ), using the mapped MLT for each identification. Figure 3b shows a comparison of the DMSP observations and model results, with  $L_{OM}$  plotted versus  $L_D$ . The mean difference in  $L$  value is  $0.893 \pm 0.602$ . The dashed line is a fit to the data and has the equation  $L_{OM} = 0.816L_D + 1.51$ . The correlation coefficient is 0.70. The larger mismatch for  $L_{OM} > 5$  may represent a breakdown in the model or the DMSP method capabilities or both. The nature of the model parameterization may introduce a bias for Dst values near 0, corresponding to extended plasmasphere conditions. The discrete values of  $L_{OM}$  near  $L = 6$  and  $L = 6.5$ , specifically, result from discontinuities from rounded Dst values. At the same time, our DMSP-based approach may have difficulty extracting PP locations when the plasmasphere is extended and diffuse.

[14] We have examined DMSP/IMAGE PP location comparisons where  $(L_I - L_D)/L_I > 0.41$  to look for any systematic explanation. We have variously examined the DMSP LIT density profiles, the relevant reprojected EUV images, and mappings of DMSP orbit tracks. Based on this review, most of these cases appear to involve periods when the plasmasphere was showing considerable structure. Half of the examples of large  $L$  differences occurred within a few hours on days 91, 92, and 101. For these cases the EUV images are suggestive of plasmasphere density structures or

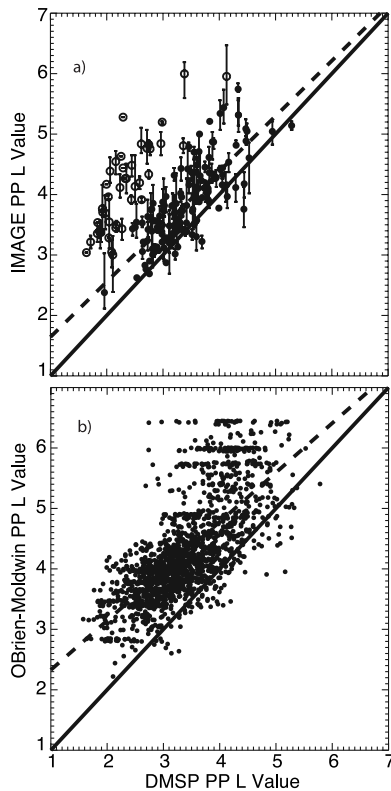


**Figure 3.** (a)  $L_I$  versus  $L_D$ . Open/solid circles indicate where  $(L_I - L_D)/L_I$  was greater/less than 0.41. The solid line represents a one-to-one correspondence while the dashed line is a fit to the solid circles. (b)  $L_{OM}$  versus  $L_D$ . The solid line represents a one-to-one correspondence while the dashed line is a fit to the data.

irregularities. For nine passes on days 128–137, the EUV images show plumes or other structures.

[15] Figure 4a illustrates one of these comparisons. The left plots show DMSP  $H^+$  density observations from four satellite passes; for one of them (F15), the L difference between the DMSP and the IMAGE derived PP is 1.5L. The four passes are within a 50-minute period, and the vertical red lines indicate the PP boundaries identified by the method described previously. The plot on the right shows the mapped orbit tracks for the four DMSP passes overlaid on a reprojected EUV image. The F15 PP maps to a notch, while the F14 and F12 PP locations are outside the notch on opposite sides. There is no significant structure in the PP on the morning side where the F13 PP location agrees very well with the IMAGE PP location.

[16] Figure 4b shows two more examples of poor comparisons within about an hour UT of each other. In each case there is a bump in the DMSP  $H^+$  density measurements poleward of LIT indicative of plasmaspheric structure. The EUV images also show the presence of plasmaspheric structure along the projected DMSP orbit tracks. The darker “bite out” seen on the left side of the images is the Earth’s shadow and the horizontal striping results from the use of three cameras to produce the single image.

[17] Examination of the comparisons where  $(L_I - L_D)/L_I > 0.41$  thus suggests that our DMSP measurements are often

identifying physical structures in the plasmasphere. We have consequently added an option to the algorithm to permit identification of multiple boundaries associated with such structures. This will enhance the usefulness of the database, e.g., identification of plumes is useful given their expected strong influence on radiation belt populations during stormtimes.

### 3. Discussion and Conclusions

[18] We have developed a preliminary method for extracting the ionospheric projection of the PP from DMSP measurements of the  $H^+$  density in the topside ionosphere. Comparisons with EUV images of the plasmasphere acquired by the IMAGE spacecraft show good agreement. We find that during the 72-day period of this study, our PP locations are on average 0.435 L earthward of the EUV PP locations. This could be a result of differences in IMAGE and DMSP location identification as well as physical processes. For instance, we developed our algorithm for identification of DMSP PP locations with the goal that it be semi-automated; manual identification typically picks out a PP location poleward of where the semi-automated algorithm identified the PP.

[19] Our PP identifications occur in the topside ionosphere. We thus need to ask, does the PP map along field lines to the equator? *Yizengaw et al.* [2005] used tomographic imaging of GSP measurements along with IMAGE data to show that the mid-latitude trough tilts equatorward in the F-region and topside ionosphere (up to 1000 km) in concert with the magnetic field lines mapped from the equatorial PP, indicating that the PP does map closely along field lines. However, they suggest that the LIT may be shifted to lower latitudes at higher altitudes compared to the mid-latitude trough since the  $H^+$  upward flow becomes stronger in the mid-latitude regions where the magnetic field inclination is greater.

[20] There could also be  $H^+$  temperature effects. The PP is often identified by a strong gradient with L value in the plasma density as in this study; the PP location is selected somewhere on that gradient, often at the high-latitude/high-L value region where that gradient goes nearly to zero, i.e., at the equatorial edge of the LIT. If the  $H^+$  temperature varies with latitude in the ionosphere, the  $H^+$  scale height will in turn vary and the density profile will change with altitude. We often see the  $H^+$  temperature increasing with latitude in the mid-latitude ionosphere across the equatorial side of the LIT; this would lead to a movement of the PP gradient to a higher L value as it is mapped to the equator. We will continue our research comparing the DMSP PP locations with all available IMAGE EUV data as well as other sources of PP identification, developing a robust algorithm for identifying the PP from the DMSP  $H^+$  density data, and examining the effect of latitudinal variations in the  $H^+$  temperature.

[21] Even if the PP as identified in the topside ionosphere does not map perfectly along constant L shells to the equatorial plane, our results show that the offset is relatively constant and the PP location in the ionosphere varies in a similar fashion to its variation in the equatorial plane. The extremely large database provided by the DMSP satellites (7 satellites over ~16 years) is a tremendous resource

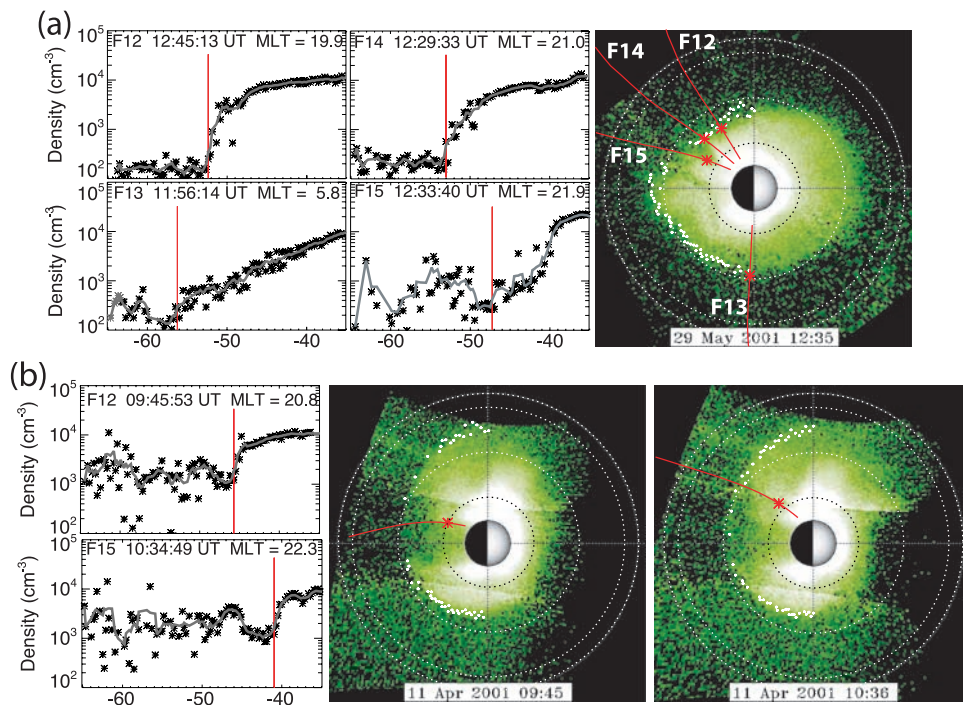


**Figure 4.** (a) The plots on the left side show DMSP  $H^+$  density observations from four satellite passes on 29 May 2001. The vertical red lines indicate the identified PP locations. The image on the right side is the IMAGE EUV observation of the plasmaspheric  $He^+$  density around the time of the DMSP passes with the DMSP orbit tracks and identified PP locations as in Figure 2. (b) Similar plots to Figure 4a for two DMSP passes on 11 April 2001.

for investigating the evolution and dynamics of the PP. In combination with energetic particle measurements from SAMPEX, available continuously since 1992, these measurements provide an extremely useful database from which to investigate the effect of the location of the PP on the processes responsible for the energization and loss of radiation belt particles in the outer zone.

[22] **Acknowledgments.** The work by P. Anderson was supported by NASA grant NNX07AG39G and the work by W. Johnston was supported by NASA grants NNX07AG39G and NNX07AU71H. We gratefully acknowledge Fred Rich for providing access to the DMSP data.

## References

- Baker, D. N., et al. (2004), An extreme distortion of the Van Allen belt arising from the ‘Halloween’ solar storm in 2003, *Nature*, *432*, 878, doi:10.1038/nature03116.
- Foster, J. C., C. G. Park, L. H. Brace, J. R. Burrows, J. H. Hoffman, E. J. Maier, and J. H. Whitteker (1978), Plasmapause signatures in the ionosphere and magnetosphere, *J. Geophys. Res.*, *83*, 1175.
- Goldstein, J., M. Spasojević, P. H. Reiff, B. R. Sandel, W. T. Forrester, D. L. Gallagher, and B. W. Reinisch (2003), Identifying the plasmapause in IMAGE EUV data using IMAGE RPI in situ steep density gradients, *J. Geophys. Res.*, *108*(A4), 1147, doi:10.1029/2002JA009475.
- Goldstein, J., S. G. Kanekal, D. N. Baker, and B. R. Sandel (2005), Dynamic relationship between the outer radiation belt and the plasmapause during March–May 2001, *Geophys. Res. Lett.*, *32*, L15104, doi:10.1029/2005GL023431.
- Grebowsky, J. M., et al. (1976), Coincident observations of ionospheric trough and the equatorial plasmapause, *Planet. Space Sci.*, *24*, 1177.
- Grebowsky, J. M., et al. (1978), Ionospheric and magnetospheric “plasmapauses,” *Planet. Space Sci.*, *26*, 651.
- Home, R. B. (2002), The contribution of wave-particle interactions to electron loss and acceleration in the Earth’s radiation belts during geomagnetic storms, in *The Review of Radio Science, 1999–2002*, edited by W. R. Stone, chap. 33, p. 801, John Wiley, Hoboken, N. J.
- Jordanova, V. K., J. U. Kozyra, A. F. Nagy, and G. V. Khazanov (1997), Kinetic model of the ring current-atmosphere interactions, *J. Geophys. Res.*, *102*, 14,279.
- Koons, H. C., and J. L. Roeder (1990), A survey of equatorial magnetospheric wave activity between 5 and 8  $R_E$ , *Planet. Space Sci.*, *38*, 1335.
- O’Brien, T. P., and M. B. Moldwin (2003), Empirical plasmapause models from magnetic indices, *Geophys. Res. Lett.*, *30*(4), 1152, doi:10.1029/2002GL016007.
- Park, C. G., and P. M. Banks (1974), Influence of thermal plasma flow on the mid-latitude nighttime  $F_2$  layer: Effects of electric fields and neutral winds inside the plasmasphere, *J. Geophys. Res.*, *79*, 4661.
- Summers, D., R. M. Thorne, and F. Xiao (1998), Relativistic theory of wave-particle resonant diffusion with application to electron acceleration in the magnetosphere, *J. Geophys. Res.*, *103*, 20,487.
- Taylor, H. A., Jr., and W. J. Walsh (1972), The light-ion trough, the main trough, and the plasmapause, *J. Geophys. Res.*, *77*, 6716.
- Yizengaw, E., and M. B. Moldwin (2005), The altitude extension of the mid-latitude trough and its correlation with plasmapause position, *Geophys. Res. Lett.*, *32*, L09105, doi:10.1029/2005GL022854.
- Yizengaw, E., H. Wei, M. B. Moldwin, D. Galvan, L. Mandrake, A. Mannucci, and X. Pi (2005), The correlation between mid-latitude trough and the plasmapause, *Geophys. Res. Lett.*, *32*, L10102, doi:10.1029/2005GL022954.

P. C. Anderson and W. R. Johnston, W. B. Hanson Center for Space Sciences, University of Texas at Dallas, P.O. Box 830688, Richardson, TX 75083, USA. (phillip.anderson1@utdallas.edu)

J. Goldstein, Space Science and Engineering Division, Southwest Research Institute, 6220 Culebra Road, San Antonio, TX 78238, USA.